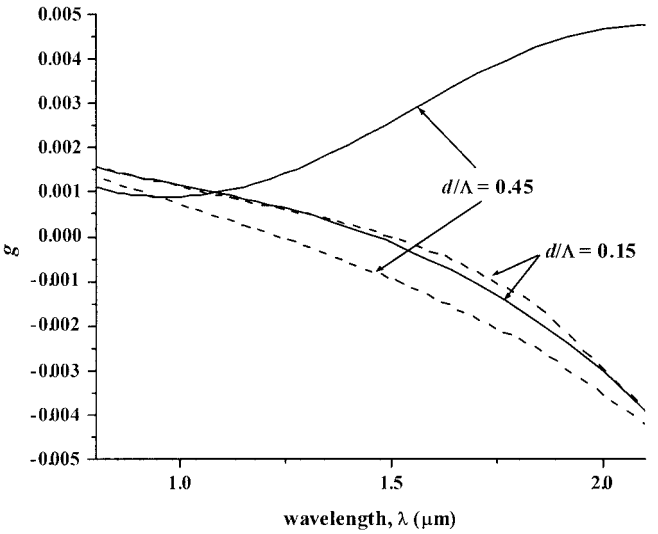

Figure 5 Total normalized GVD obtained by analytically evaluating the sum of material and waveguide dispersion (dashed lines) and by numerical differentiation (solid lines)

of the core and cladding are very similar" [6]. As observed from Figure 3, this is only true for photonic-crystal fiber with small hole diameters. The validity of this approach may therefore become questionable for larger hole diameters.

More accurate results may be obtained by using numerical differentiation to investigate the dispersion properties of photonic-crystal fibers. Using values of n_1 obtained by the Sellmeier equation and corresponding values of $n_{2\text{eff}}$ (Fig. 3), the values of propagation constant β are calculated for different wavelengths using step-index fiber theory. The values of $(\beta\Lambda)$ against $(k\Lambda)$ are modeled using a piecewise polynomial interpolation of order 3. The normalized GVD in Eq. (3) is then obtained by differentiating the interpolating polynomials. This procedure includes the effect of dispersion in silica and does not need the addition of material dispersion. Since no other approximations are used, the validity of results obtained in this way is only limited by the degree of accuracy to which the values of β have been computed.

Figure 5 shows the calculated results using the two different approaches. The plots are given for the range of wavelength of interest in current optical-fiber communication systems. Moreover, outside this range of wavelength, the material (silica) dispersion predominates over waveguide dispersion.

It may be observed that the normalized GVD calculated by both procedures agree for small hole diameter, but not for larger holes. This confirms the fact that the separation of normalized GVD into the two components, as in Eq. (4), is only valid for a limited range of hole diameters. The cause can be seen by examining the variation of the refractive index of silica and that of the effective refractive index with wavelength shown in Figure 3. For small hole diameter, the variation of effective refractive index with wavelength closely follows that of the refractive index of silica. However, for larger holes, the variation of effective index with wavelength diverts from that of the refractive index of silica, thus violating the principle upon which the separation is based [6].

CONCLUSION

Most of the reported research on photonic-crystal fibers uses a nominal refractive index of silica, such as the "vector methods" in [3, 7]. However, we note that in [7] material dispersion was included by using an iterative algorithm and the standard Sellmeier equation for calculating dispersion characteristics of a photonic-crystal fiber.

In this paper, the separation of normalized GVD was shown to be valid only for small hole diameters, in which case the variation of the effective index closely follows that of the wavelength-dependent refractive index of silica. It was further demonstrated that, for a more accurate analysis encompassing a much wider range of hole diameters, the wavelength-dependent refractive index of silica needs to be taken into account in all calculations.

REFERENCES

1. T.A. Birks, J.C. Knight, and P.St.J. Russel, Endlessly single-mode photonic crystal fiber, Optics Lett 22 (1997), 961–963.
2. D. Mogilevtsev, T.A. Birks, and P.St.J. Russel, Group-velocity dispersion in photonic crystal fibers, Optics Lett 23 (1998), 1662–1664.
3. A. Ferrando, E. Silvestre, J.J. Miret, and P. Andres, Full-vector analysis of a realistic photonic crystal fiber, Optics Lett 24 (1999), 276–278.
4. R.K. Sinha and S.K. Varshney, Dispersion properties of photonic crystal fibers, Microwave Opt Technol Lett 37 (2003), 129–132.
5. I.H. Malitson, Interspecimen comparison of the refractive index of fused silica, J Optics Soc Am 55 (1965), 1205–1209.
6. D. Gloge, Dispersion in weakly guiding fibers, Appl Optics 10 (1971), 2442–2445.
7. D. Ouzonov, D. Homoelle, W. Zipfel, W.W. Webb, A.L. Gaeta, J.A. West, J.C. Fajardo, and K.W. Koch, Dispersion measurements of microstructured fibers using femtosecond laser pulses, Optics Commun 192 (2001), 219–223.

A LOW-LOSS WIDEBAND SUSPENDED COAXIAL TRANSMISSION LINE

I. Llamas-Garro,[1]* M. J. Lancaster,[2] and P. S. Hall[2]
[1] Laboratory for Microsensors & Actuators
School of Electrical Engineering and Computer Science Seoul National University
Kwanak P.O. Box 34
Seoul 151-600, South Korea
[2] School of Electronic, Electrical and Computer Engineering
The University of Birmingham
B15-2TT, United Kingdom

Received 3 April 2004

ABSTRACT: *This paper presents a transmission-line structure suitable for micromachining technology. The structure is an air-filled square coaxial cable, which is very low loss and has been designed in order to utilise current manufacturing processes. This transmission line demonstrates that such a structure can be designed to cover very wide bandwidth. As the cable is air filled, the centre conductor needs to be supported and this is accomplished by attaching quarter-wavelength stubs to the ground. The design method of such a cable is presented in detail and the results of an X-band component are presented.* © 2004 Wiley Periodicals, Inc. Microwave Opt Technol Lett 43: 93–95, 2004; Published online in Wiley InterScience (www.interscience.wiley.com). DOI 10.1002/mop.20386

Key words: *coaxial transmission lines; microwave filters; millimetre waves*

1. INTRODUCTION

Today's communications systems have a huge variety of carrier frequencies where communications have traditionally been based

* I. Llamas-Garro's current affiliation is Seoul National University, Seoul, South Korea.

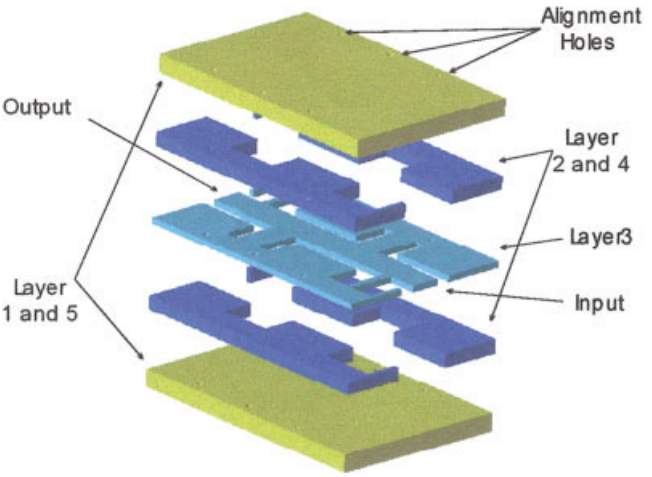

Figure 1 Assembly of the self-supported coaxial transmission line. [Color figure can be viewed in the online issue, which is available at www.interscience.wiley.com.]

at frequencies around and below 2 GHz; however, it is now common place to have systems based on many tens of gigahertz. There are various types of technology for implementing these systems and micromachined components are seen as a potential candidate for low-cost, high-performance, receiver front ends. The high precision of the micromachining is useful when the wavelengths become short. For all front-ends, the most important component to consider is the basic transmission line or waveguide that interconnects the various parts of the system and must be a convenient structure for interface with other components as well as having low loss. Several structures have been proposed over the last few years, including a dielectric-filled coaxial line [1], suspended coplanar line [2–4], and air-filled microstrip [5, 6] or inverted microstrip lines [7, 8].

Here, we propose a square coaxial cable for use with micromachining technology; such a cable is one of the lowest loss structures for a given cross section. The proposed cable is air filled, so that dielectric losses play no role in the attenuation. Additionally, there is no radiation loss or cross coupling with other parts of the circuit. A wideband transmission line is demonstrated at around the X-band, but the intention is for the designs to be used at much higher frequencies with construction out of laser machined metal [9], metal-coated thick resists such as SU8 [3, 6] or metal-coated plasma-etched silicon wafers [10, 11]. One obvious problem is that if the cable is air filled, how is the coaxial cable's centre conductor held up? This is achieved by quarter-wavelength stubs which go from the centre conductor to the outer conductor at appropriate intervals along the length of the cable. Of course, this has a band-limiting effect, but the design described below maximises this bandwidth.

Figure 1 shows the construction of the cable. It is made of five separate layers to allow for the micromachined construction processes. The central layer, marked layer 3 in Figure 1, is the centre conductor of the coaxial cable and the stubs can be seen connecting this to the outer ground, which is on the same level. Layers 2 and 4 are the ground layers, with layers 1 and 5 forming the top and bottom ground of the square coaxial structure, respectively. Once these five layers are bonded together, a fully enclosed self-suspended coaxial structure is formed.

The coaxial cable can be designed for wideband use. The best way to do this and include the effects of the stubs is to use a conventional filter-design technique, thus making the filter bandwidth as wide as possible. This gives precise control over the ripple and bandwidth of the coaxial cable. A simple Chebycheff response is chosen. In order to minimise loss, it is important to have a large cable cross section; however, there comes a point where nonTEM modes begin to propagate [12, 13], and this therefore limits the size. The particular filter demonstrated in this paper has a centre frequency of 9 GHz with a 0.01-dB passband ripple, and a 70% fractional bandwidth. The frequency at which the nonTEM modes occur is 13 GHz. Although this particular cable is at the X-band, a filter using these ideas has been produced at 29.75 GHz for local-area multipoint distribution systems [9].

TABLE 1 Design Parameters for the Suspended Coaxial Transmission Line

Low-Pass Prototype g Values			
$g_1 = 0.7128$,	$g_2 = 1.2003$,	$g_3 = 1.3212$,	$g_4 = 0.6476$, $g_5 = 1.1007$
Characteristic Impedances of the Shunt Stubs			
$Z_1 = 99.179$	$Z_2 = 50.241$	$Z_3 = 50.24$	$Z_4 = 99.174$
Characteristic Impedances of the Connecting Lines			
$Z_{12} = 45.879$	$Z_{23} = 44.167$		$Z_{34} = 45.88$

2. WIDEBAND TRANSMISSION LINE DESIGN

A general quarter-wavelength stub-supported transmission-line filter can be designed starting with a low-pass prototype filter. A band-pass transformation can then be applied to obtain the band-pass filter, which is implemented physically as shorted quarter-wavelength stubs connected by quarter-wavelength transmission lines. The design formulas and the general procedure to calculate the impedance required for the different transmission line sections are described in [14]. Table 1 contains all the resulting impedances involved in the design and the low-pass prototype g values used. The centre frequency for the design is 9 GHz, with a 70% fractional bandwidth, having four poles with 0.01-dB passband ripple, and a Chebycheff response.

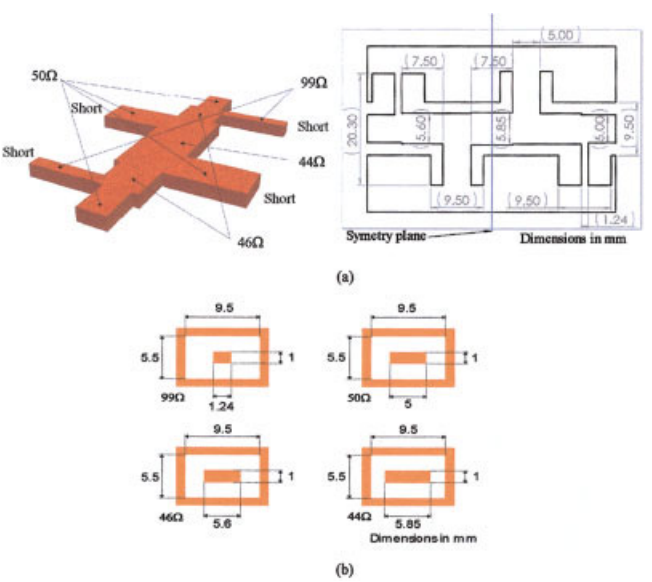

Figure 2 Suspended coaxial transmission line supported by stubs: (a) center conductor only and the dimensions of layer 3; (b) cross section of the different impedance coaxial transmission-line sections. [Color figure can be viewed in the online issue, which is available at www.interscience.wiley.com.]

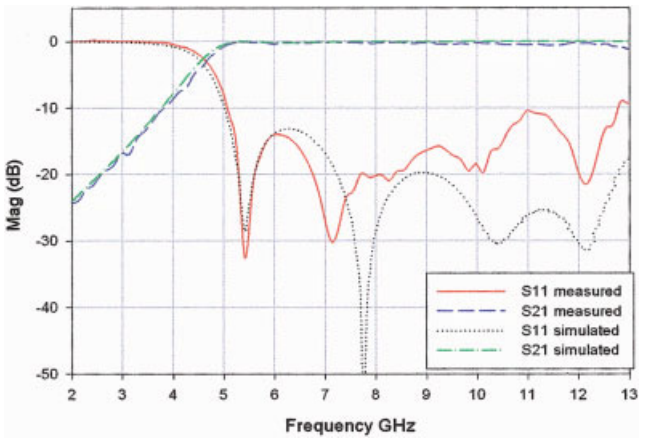

Figure 3 Response of the suspended coaxial transmission line. [Color figure can be viewed in the online issue, which is available at www.interscience.wiley.com.]

The different impedances needed for the suspended coaxial transmission line can be achieved by varying the size of the centre conductor [15]; here, the size of the outer conductor is fixed. The centre conductor of the resulting suspended coaxial transmission line is shown in Figure 2(a), with the cross-sections of the 50Ω line and the stubs shown in Figure 2(b). The input and output of the suspended transmission line, as shown in Figure 1, consist of 50Ω sections of transmission line.

For the coaxial assembly shown in Figure 1, layer 3 is 1-mm thick, and layers 2 and 4 are 2.25-mm thick. The complete device has an enclosed overall dimension of 45 × 20 × 5.5 mm. The five layers were clamped together for the experimental results given as follows.

3. RESULTS

The response of the suspended coaxial transmission line is shown in Figure 3; good agreement between theory and experiment is obtained. The transmission line was designed to work up to 13 GHz in a TEM mode; beyond this frequency, higher modes propagate through the structure, thus leading to a dispersive coaxial line. The suspended coaxial transmission line presented has low-loss transmission, and a usable frequency range from 5 to 13 GHz. The simulations were done according to [16]. The deviation of S_{11} from the simulations at the higher frequencies is probably due to a slight layer misalignment.

4. CONCLUSION

The layered air-filled coaxial cable discussed in this paper is a compact transmission line suitable for manufacture using micromachining technologies. The cable has been successfully demonstrated at the X-band, showing a low-loss wideband cable made out of five conducting layers. It is important to note that the structure allows the possibility of integrating other 3D structures made out of planar machined layers, such as filters, coupling structures, phase shifters, antennas, and delay lines.

REFERENCES

1. J.A. Bishop, M.M. Hashemi, K. Kiziloglu, L. Larson, N. Dagli, and U. Mishra, Monolithic coaxial transmission lines for mm-wave ICs, High speed semiconductor devices and circuits, Proc IEEE/Cornell Conf Adv Concepts, Ithaca, NY, 1991, pp. 252–260.
2. K.J. Herrick, T.A. Schwartz, and L.P.B. Katehi, Si-micromachined coplanar waveguides for use in high-frequency circuits, IEEE Trans Microwave Theory Tech 46 (1998), 762–768.
3. W.Y. Liu, D.P. Steenson and M.B. Steer, Membrane-supported CPW with mounted active devices, IEEE Microwave Wireless Compon Lett 11 (2001), 167–169.
4. J.-H. Park, C.-W. Baek, S. Jung, H.-T. Kim, Y. Kwon, and Y.-K. Kim, Novel micromachined coplanar waveguide transmission lines for application in millimetre-wave circuits Jpn J Appl Phys 39 (2000), 7120–7124.
5. P. Blondy, A.R. Brown, D. Cross and G.M. Rebeiz, Low-loss micromachined filters for millimetre-wave telecommunication systems, IEEE MTT-S Dig, Baltimore, MD (1998), 1181–1184.
6. J.E. Harriss, L.W. Pearson, X. Wang, C.H. Barron, and A.V. Pham, Membrane-supported Ka band resonator employing organic micromachined packaging, IEEE MTT-S Dig, Boston, MA (2000), 1225–1228.
7. H. Henri, S. Gonzague, V. Matthieu, C. Alain, and D. Gilles, Ultra low-loss transmission lines on low resistivity silicon substrate, IEEE MTT-S Dig, Boston, MA (2000), 1809–1812.
8. K. Takahashi, U. Sangawa, S. Fujita, M. Matsuo, T. Urabe, H. Ogura, and H. Yabuki, Packaging using microelectromechanical technologies and planar components, IEEE Trans Microwave Theory Tech 49 (2001), 2099–2104.
9. I. Llamas-Garro, K. Jiang, P. Jin, and M.J. Lancaster, SU-8 microfabrication for a Ka band filter, 4th Wkshp MEMS Millimiterwave Commun, Toulouse, France, 2003, pp. F55–F58.
10. S. Shimizu, K. Kuribayashi, M. Ohno, T. Taniguchi, and T. Ueda, Low-temperature reactive ion etching for bulk micromachining, IEEE Symp Emerging Technologies and Factory Automation, 1994, pp. 48–52.
11. C. Marxer, N.F. de Rooij, Micro-opto-mechanical 2 × 2 switch for single-mode fibers based on plasma-etched silicon mirror and electrostatic actuation. J Lightwave Tech 17 (1999), 2–6.
12. L. Gruner, Higher order modes in square coaxial lines, IEEE Trans Microwave Theory Tech 31 (1983), 770–772.
13. L. Gruner, Higher order modes in rectangular coaxial waveguides, IEEE Trans Microwave Theory Tech MTT-15 (1967), 483–485.
14. J.-S. Hong and M.J. Lancaster, Microstrip filters for RF/Microwave applications, Wiley, New York, 2001.
15. T.-S. Chen, Determination of the capacitance, inductance, and characteristic impedance of rectangular lines, IRE Trans Microwave Theory Tech 8 (1960), 510–519.
16. Ansoft HFSS. http://www.ansoft.com.

DUAL-FREQUENCY-SELECTIVE SURFACES FOR NEAR-INFRARED BANDPASS FILTERS

S. Govindaswamy,[1] J. East,[1] F. Terry,[1] E. Topsakal,[2] J. L. Volakis,[3] and G. I. Haddad[1]
[1] Solid State Electronics Laboratory
Electrical Engineering and Computer Science Department
University of Michigan
Ann Arbor, MI 48109
[2] Department of Electrical and Computer Engineering
Mississippi State University
Mississippi State, MS 39762
[3] Radiation Laboratory
Electrical Engineering and Computer Science Department
University of Michigan
Ann Arbor, MI 48109

Received 8 April 2004

ABSTRACT: *A bandpass filter resonating at ~1.4 μm and based on a dual-frequency-selective surface design is fabricated and characterized on a silicon substrate. The filter consists of square apertures arranged*

J.L. Volakis is also a Professor and the Director of ElectroScience Laboratory, Electrical Engineering Department, The Ohio State University, Columbus, OH 43212. E. Topsakal was formerly with the University of Michigan.